Characterization of Zirconium Sulfate Supported on Zirconia and Activity for Acid Catalysis

Jong Rack Sohn,[*] Tae-Dong Kwon,[†] and Sang-Bock Kim[†]

Department of Industrial Chemistry, Engineering College, Kyungpook National University, Taegu 702-701, Korea
[†]Department of Chemistry, University of Ulsan, Ulsan 680-749, Korea
Received August 24, 2001

Zirconium sulfate supported on zirconia catalysts were prepared by impregnation of powdered $Zr(OH)_4$ with zirconium sulfate aqueous solution followed by calcining in air at high temperature. The characterization of prepared catalysts was performed using Fourier transform infrared (FTIR), X-ray diffraction (XRD), differential scanning calorimetry (DSC), and by the measurement of surface area. The addition of zirconium sulfate to zirconia increased the phase transition temperature of ZrO_2 from amorphous to tetragonal due to the interaction between zirconium sulfate and zirconia, and the specific surface area and acidity of catalysts increased in proportion to the zirconium sulfate content up to 10 wt % of $Zr(SO_4)_2$. Infrared spectra of ammonia adsorbed on $Zr(SO_4)_2/ZrO_2$ showed the presence of Brönsted and Lewis acid sites on the surface. 10-$Zr(SO_4)_2/ZrO_2$ calcined at 600 °C exhibited maximum catalytic activities for 2-propanol dehydration and cumene dealkylation. The catalytic activities for both reactions were correlated with the acidity of catalysts measured by ammonia chemisorption method.

Keywords : Zirconium sulfate, Acid catalysis, 2-Propanol dehydration, Cumene dealkylation.

Introduction

It is known that the activity of a catalyst is greatly influenced by the method of catalyst preparation and the conditions of pretreatment.[1-4] This is illustrated by the fact that the physical or chemical structure of a catalyst varies with the method of preparation, and that chemical species adsorbed on the surface affect the catalytic activity profoundly. The strong acidity of zirconia-supported sulfate has attracted much attention because of its ability to catalyze many reactions such as cracking, alkylation, and isomerization. The potential for a heterogeneous catalyst has yielded many papers on the catalytic activity of sulfated zirconia materials.[5-9] Sulfated zirconia incorporating Fe and Mn has been shown to be highly active for butene isomerization, catalyzing the reaction even at room temperature.[10,11]

It has been reported by several workers that the addition of platinum to zirconia modified by sulfate ions enhances catalytic activity in the skeletal isomerization of alkanes without deactivation when the reaction is carried out in the presence of hydrogen.[12-14] The high catalytic activity and small deactivation can be explained by both the elimination of the coke by hydrogenation and hydrogenolysis,[12] and the formation of Brönsted acid sites from H_2 on the catalysts.[13] Recently, Hino and Arata reported zirconia-supported tungsten oxide as an alternative material in reaction requiring strong acid sites.[5,15] Several advantages of tungstate, over sulfate, as dopant include that it does not suffer from dopant loss during thermal treatment and it undergos significantly less deactivation during catalytic reaction.[16]

On the other hand, many metal sulfates generate fairly large amounts of acid sites of moderate or strong strength on their surfaces when they are calcined at 400-700 °C.[4,17] The acidic property of metal sulfate often gives high selectivity for diversified reactions such as hydration, polymerization, alkylation, cracking, and isomerization.[4,17] However, structural and physicochemical properties of supported metal sulfates are considered to be in different states compared with bulk metal sulfates because of their interaction with supports.[18,19] Zirconium sulfate catalysts supported on zirconia have not been reported up to now.

This paper describes the characterization of zirconium sulfate supported on zirconia and its activity for acid catalysis. The characterization of the samples was performed by means of Fourier transform infrared (FTIR), X-ray diffraction (XRD), differential scanning calorimetry (DSC), and surface area measurements. For the acid catalysis, the 2-propanol dehydration and cumene dealkylation were used as test reactions.

Experimental Section

Catalyst preparation. The precipitate of $Zr(OH)_4$ was obtained by adding aqueous ammonia slowly into an aqueous solution of zirconium oxychloride (Junsei Chemical Co.) at room temperature with stirring until the pH of mother liquor reached about 8. The precipitate thus obtained was washed thoroughly with distilled water until chloride ion was not detected, and was dried at room temperature for 12 h. The dried precipitate was powdered below 100 mesh.

The catalysts containing various zirconium sulfate (Kanto Chemical Co.) contents were prepared by adding an aqueous solution of zirconium sulfate [$Zr(SO_4)_2 \cdot 4H_2O$] to the $Zr(OH)_4$ powder followed by drying and calcining at high temperatures for 2 h in air. This series of catalysts are denoted by their weight percentage of $Zr(SO_4)_2$. For example,

5-$Zr(SO_4)_2/ZrO_2$ indicates the catalyst containing 5 wt % $Zr(SO_4)_2$.

Characterization. FTIR spectra were obtained in a heatable gas cell at room temperature using Mattson Model GL6030E FTIR spectrophotometer. The self-supporting catalyst wafers contained about 9 mg/cm^2. Prior to obtaining the spectra the samples were heated under vacuum at 400-500 ^oC for 1.5 h.

Catalysts were checked in order to determine the structure of the catalysts by means of a Philips X'pert-APD X-ray diffractometer, employing Cu Kα (Ni-filtered) radiation.

DSC measurements were performed in air by a PL-STA model 1500H apparatus, and the heating rate was 5 ^oC per minute. For each experiment 10-15 mg of sample was used.

The specific surface area was determined by applying the BET method to the adsorption of N_2 at −196 ^oC. Chemisorption of ammonia was also employed as a measure of the acidity of catalysts. The amount of chemisorption was determined based on the irreversible adsorption of ammonia.[20-22]

2-propanol dehydration was carried out at 160-180 ^oC in a pulse micro-reactor connected to a gas chromatograph. Fresh catalyst in the reactor made of 1/4 inch stainless steel was pretreated at 400 ^oC for 1 h in the nitrogen atmosphere. Diethyleneglycol succinate on Shimalite was used as packing material of gas chromatograph and the column temperature was 150 ^oC for analyzing the product. Catalytic activity for 2-propanol dehydration was represented as mole of propylene converted from 2-propanol per gram of catalyst. Cumene dealkylation was carried out at 350-400 ^oC in the same reactor as above. Packing material for the gas chromatograph was Benton 34 on chromosorb W and column temperature was 130 ^oC. Catalytic activity for cumene dealkylation was represented as mole of benzene converted from cumene per gram of catalyst. Conversion for both reactions were taken as the average of the first to sixth pulse values.

Results and Discussion

Infrared spectra. The IR spectra of 10-$Zr(SO_4)_2/ZrO_2$ (KBr disc) calcined at different temperatures (400-800 ^oC) are given in Figure 1. 10-$Zr(SO_4)_2/ZrO_2$ calcined up to 700 ^oC showed IR absorption bands at 1205, 1112, 1063 and 1019 cm^{-1} which are assigned to bidentate sulfate ion coordinated to the metal such as Zr^{4+}.[22] However, for the calcination of 800 ^oC IR bands by the sulfate ion disappeared due to the complete decomposition of sulfate ion, as shown in Figure 1. These results are in good agreement with those of thermal analysis described later.

In general, for the metal oxides modified with sulfate ion followed by evacuating above 400 ^oC, a strong band assigned to S=O stretching frequency is observed at 1380-1370 cm^{-1}.[23-25] In this work, the corresponding band for samples exposed to air was not found because water molecules in air were adsorbed on the surfaces of catalysts. These results are very similar to those reported by other authors.[23-25] However, in a separate experiment IR spectrum of self-supported 10-$Zr(SO_4)_2/ZrO_2$ after evacuation at 400 ^oC for 2 h was examined, so that there was an intense band at 1376 cm^{-1} accompanied by broad and intense bands below 1250 cm^{-1} due to the overlapping of the ZrO_2 skeletal vibration, indicating the presence of different adsorbed species depending on the treatment conditions of the sulfated sample.[24]

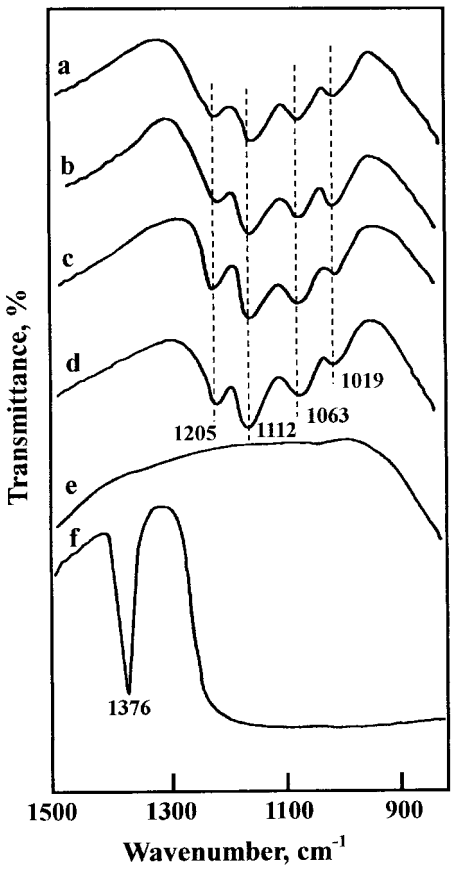

Figure 1. Infrared spectra of 10-$Zr(SO_4)_2/ZrO_2$ calcined at different temperatures for 2 h; (a) 400 ^oC, (b) 500 ^oC, (c) 600 ^oC, (d) 700 ^oC, (e) 800 ^oC, and (f) after evacuation at 400 ^oC for 2 h.

Crystalline structures of catalysts. The crystalline structures of catalysts calcined in air at different temperatures for 2 h were examined. In the case of zirconia support, as shown in Figure 2, ZrO_2 was amorphous to X-ray diffraction up to 300 ^oC, with a tetragonal phase at 350 ^oC, a two-phase mixture of the tetragonal and monoclinic forms at 400-800 ^oC, and a monoclinic phase at 900 ^oC. Three crystal structures of ZrO_2, *i.e.*, tetragonal, monoclinic, and cubic phases have been reported.[26,27]

However, in the case of supported zirconium sulfate catalysts the crystalline structures of the samples were different from structure of the ZrO_2, support. For the 5-$Zr(SO_4)_2/ZrO_2$, as shown in Figure 3, ZrO_2 is amorphous up to 400 ^oC. In other words, the transition temperature from the amorphous to tetragonal phase was higher by 150 ^oC than that of pure ZrO_2. X-ray diffraction data indicated a tetragonal phase of ZrO_2 at 500-600 ^oC, a two-phase mixture of the tetragonal and monoclinic ZrO_2 forms at 700 ^oC, and a monoclinic phase of ZrO_2 at 800-900 ^oC. It is assumed that the interaction between zirconium sulfate and ZrO_2 hinders the transition of

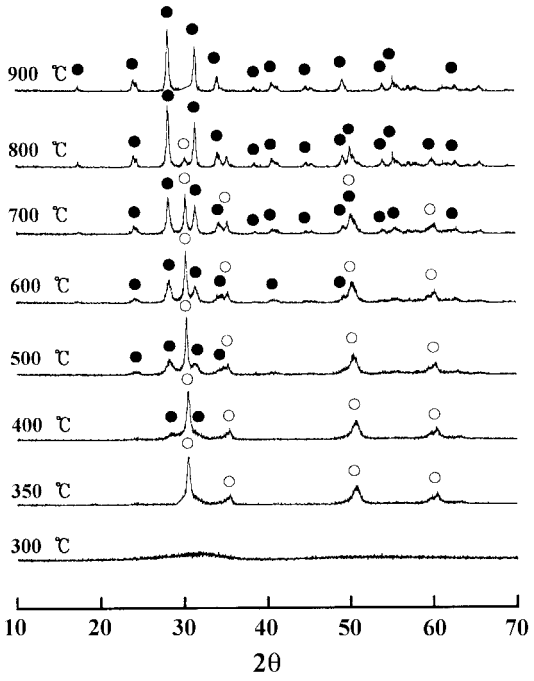

Figure 2. X-ray diffraction patterns of ZrO_2 calcined at different temperatures for 2 h: ○ , tetragonal phase of ZrO_2; ● , monoclinic phase of ZrO_2.

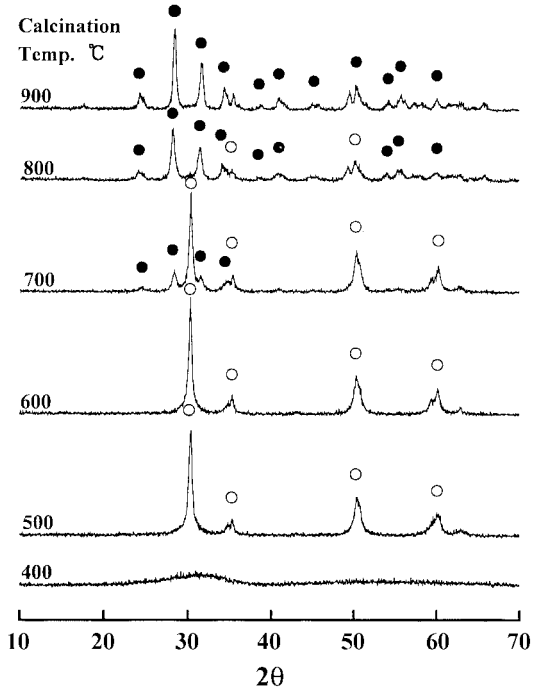

Figure 3. X-ray diffraction patterns of 5-$Zr(SO_4)_2/ZrO_2$ calcined at different temperatures for 2 h: ○ , tetragonal phase of ZrO_2; ● , monoclinic phase of ZrO_2.

ZrO_2 from amorphous to tetragonal phase.[2,28] These results are in good agreement with those of DSC described later. The presence of zirconium sulfate strongly influences the development of textural properties with temperature. For 5-$Zr(SO_4)_2/ZrO_2$, the crystalline phase of zirconium sulfate

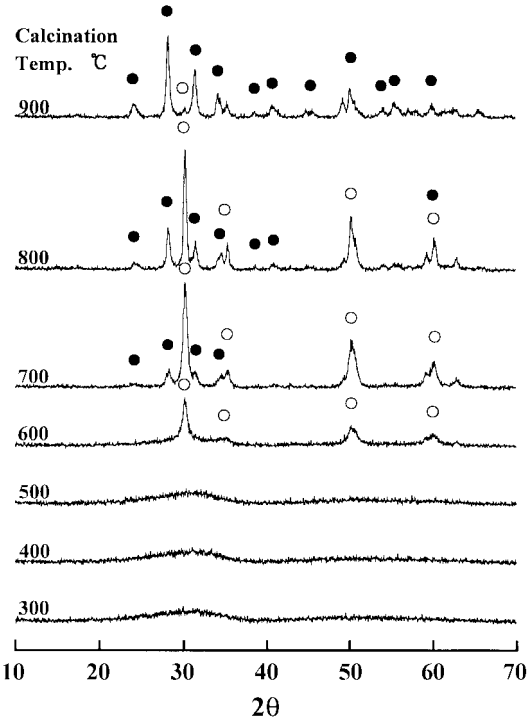

Figure 4. X-ray diffraction patterns of 15-$Zr(SO_4)_2/ZrO_2$ calcined at different temperatures for 2 h: ○ , tetragonal phase of ZrO_2; ● , monoclinic phase of ZrO_2.

was not observed at any calcination temperature, indicating that most of zirconium sulfate is present as amorphous form and the zirconium sulfate is well dispersed on the surface of zirconia.

Moreover, for the sample of 15-$Zr(SO_4)_2/ZrO_2$ the transition temperature of ZrO_2 from amorphous to tetragonal phase was higher by 250 °C than that of pure ZrO_2. That is, the more the content of zirconium sulfate, the higher the phase transition temperature. However, as shown in Figure 4, X-ray diffraction patterns of 15-$Zr(SO_4)_2/ZrO_2$ were different from those of 5-$Zr(SO_4)_2/ZrO_2$. 15-$Zr(SO_4)_2/ZrO_2$ was amorphous to X-ray diffraction up to 500 °C, with a tetragonal phase of ZrO_2 at 600 °C and a two phase mixture of the tetragonal and monoclinic forms at 700-900 °C. However, as shown in Figure 4, the amount of monoclinic phase increased with the calcination temperature, indicating the easy phase transition from tetragonal to monoclinic form at high temperature.

It is also of interest to examine the influence of zirconium sulfate on the transition temperature of ZrO_2 from tetragonal to monoclinic phase. In view of X-ray diffraction patterns, the calcination temperature at which monoclinic phase is observed initially is 400 °C for pure ZrO_2 and 700 °C for 5-$Zr(SO_4)_2/ZrO_2$ and 15-$Zr(SO_4)_2/ZrO_2$, respectively. That is, the transition temperature increases with increasing zirconium sulfate content. This can also be explained in terms of the delay of transition from tetragonal to monoclinic phase due to the interaction between zirconium sulfate and zirconia, in analogy with the delay of transition from amorphous to tetragonal phase described above.

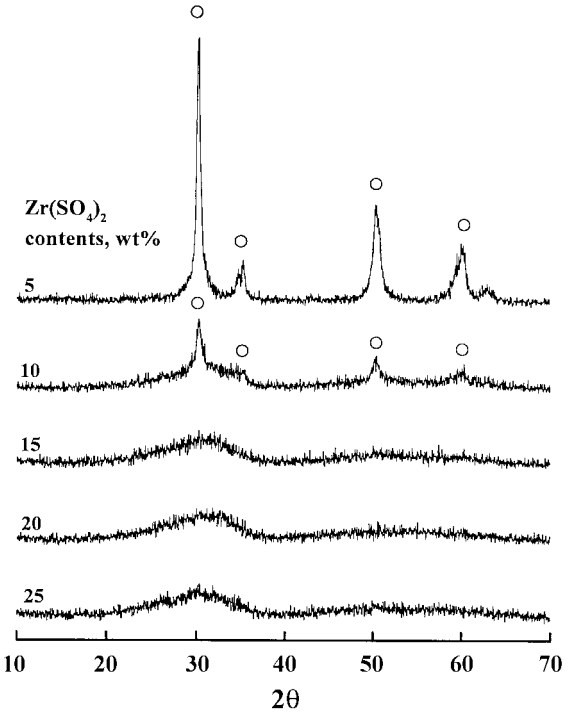

Figure 5. X-ray diffraction patterns of $Zr(SO_4)_2/ZrO_2$ having various $Zr(SO_4)_2$ contents and calcined at 500 °C for 2 h: ○ , tetragonal phase of ZrO_2; ● , monoclinic phase of ZrO_2.

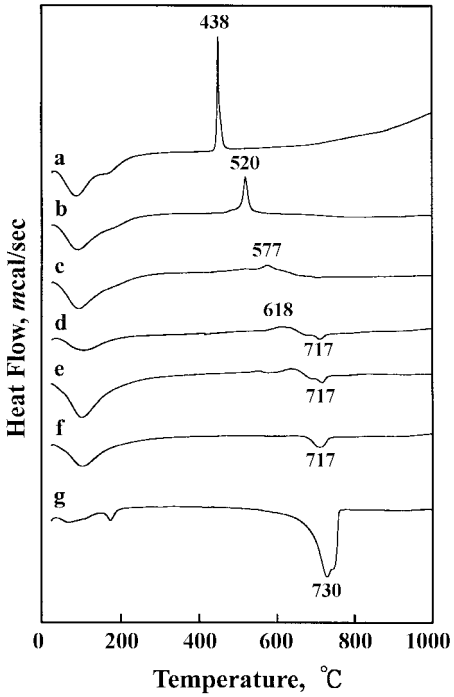

Figure 6. DSC curves of precursor for $Zr(SO_4)_2/ZrO_2$ having different $Zr(SO_4)_2$ contents; (a) ZrO_2, (b) 5-$Zr(SO_4)_2/ZrO_2$, (c) 10-$Zr(SO_4)_2/ZrO_2$, (d) 15-$Zr(SO_4)_2/ZrO_2$, (e) 20-$Zr(SO_4)_2/ZrO_2$, (f) 25-$Zr(SO_4)_2/ZrO_2$, and (g) $Zr(SO_4)_2 \cdot 4H_2O$.

The XRD patterns of $Zr(SO_4)_2/ZrO_2$ containing different zirconium sulfate contents and calcined at 500 °C for 2 h are shown in Figure 5. ZrO_2 is a tetragonal phase up to 10 wt %, but for samples containing high zirconium sulfate above 10 wt %, ZrO_2 was amorphous because the interaction between zirconium sulfate and ZrO_2 hinders the phase transition of ZrO_2 from amorphous to tetragonal phase.

Thermal analysis. The X-ray diffraction patterns in Figures 3-5 clearly showed that the structure of $Zr(SO_4)_2/ZrO_2$ was different depending on the calcined temperature. To examine the thermal properties of precusors of $Zr(SO_4)_2/ZrO_2$ samples more clearly, their thermal analysis has been carried out as illustrated in Figure 6. For pure ZrO_2, the DSC curve shows a broad endothermic peak below 180 °C due to water elimination, and a sharp and exothermic peak at 438 °C due to the ZrO_2 crystallization.[28] However, it is of interest to see the influence of zirconium sulfate on the crystallization of ZrO_2 from amorphous to tetragonal phase. As Figure 6 shows, the exothermic peak due to the crystallization appears at 438 °C for pure ZrO_2, while for $Zr(SO_4)_2/ZrO_2$ samples it is shifted to higher temperatures due to the interaction between $Zr(SO_4)_2$ and ZrO_2. The shift increases with increasing zirconium sulfate content. Consequently, the exothermic peaks appear at 520 °C for 5-$Zr(SO_4)_2/ZrO_2$, 577 °C for 10-$Zr(SO_4)_2/ZrO_2$ and 618 °C for 15-$Zr(SO_4)_2/ZrO_2$. These results are in good agreement with those of X-ray results described above. The endothermic peaks around 717-730 °C for $Zr(SO_4)_2/ZrO_2$ samples and pure $Zr(SO_4)_2$ are due to the evolution of SO_3 decomposed from sulfate ion bonded to the surface of zirconia.[18,19]

Surface properties. It is necessary to examine the effect of zirconium sulfate on the surface properties of catalysts, that is, specific surface area, acidity, and acid strength. The specific surface areas of samples calcined at 600 °C for 2 h are listed in Table 1. The presence of zirconium sulfate strongly influences the surface area in comparison with the pure ZrO_2. Specific surface areas of $Zr(SO_4)_2/ZrO_2$ samples are much larger than that of pure ZrO_2 calcined at the same temperature, showing that surface area increases gradually with increasing zirconium sulfate content up to 10 wt % of $Zr(SO_4)_2$. It seems likely that the interaction between zirconium sulfate and ZrO_2 protects catalysts from sintering.[2]

The acidity of catalysts calcined at 600 °C, as determined by the amount of NH_3 irreversibly adsorbed at 230 °C,[18-21] is listed in Table 1. As listed in Table 1, the acidity increases abruptly upon the addition of zirconium sulfate [0.5 wt % of

Table 1. Specific surface area and acidity of $Zr(SO_4)_2/ZrO_2$ calcined at 600 °C for 2 h

Catalysts	Surface area (m^2/g)	Acidity (μmol/g)
ZrO_2	56.1	41.3
0.5-$Zr(SO_4)_2/ZrO_2$	99.2	104.9
1-$Zr(SO_4)_2/ZrO_2$	109.4	108.6
3-$Zr(SO_4)_2/ZrO_2$	126.9	145.7
5-$Zr(SO_4)_2/ZrO_2$	137.9	160.3
10-$Zr(SO_4)_2/ZrO_2$	142.3	168.1
15-$Zr(SO_4)_2/ZrO_2$	124.3	137.2
20-$Zr(SO_4)_2/ZrO_2$	110.4	126.8
25-$Zr(SO_4)_2/ZrO_2$	66.2	78.7

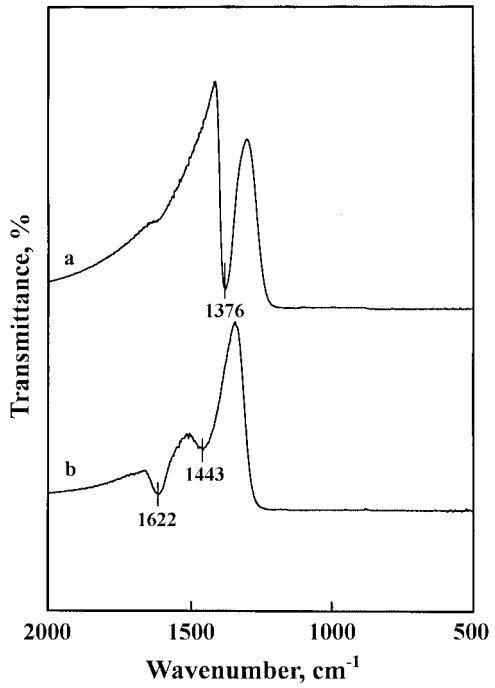

Figure 7. Infrared spectra of NH_3 adsorbed on 10-$Zr(SO_4)_2/ZrO_2$; (a) background of 10-$Zr(SO_4)_2/ZrO_2$ evacuated at 400 °C for 1 h and (b) ammonia (20 Torr) adsorbed on (a) followed by evacuating at 230 °C for 40 min.

$Zr(SO_4)_2$] to ZrO_2, and then the acidity increases very gently with increasing zirconium sulfate content up to 10 wt % of $Zr(SO_4)_2$. In view of Table 1, it is clear that the acidity runs parallel with the surface area. That is, the higher the surface area, the more the acidity.

Infrared spectroscopic studies of ammonia adsorbed on solid surfaces have made it possible to distinguish between Brönsted and Lewis acid sites.[29,30] Figure 7 shows the IR spectra of ammonia adsorbed on 10-$Zr(SO_4)_2/ZrO_2$ samples evacuated at 400 °C for 1 h. For 10-$Zr(SO_4)_2/ZrO_2$ the band at 1443 cm^{-1} is the characteristic peak of ammonium ion, which is formed on the Brönsted acid sites and the absorption peak at 1622 cm^{-1} is contributed by ammonia coordinately bonded to Lewis acid sites,[29,30] indicating the presence of both Brönsted and Lewis acid sites on the surface of 10-$Zr(SO_4)_2/ZrO_2$ sample. Other samples having different zirconium sulfate content also showed the presence of both Lewis and Brönsted acids. As Figure 7(a) shows, the intense band at 1376 cm^{-1} after evacuation at 400 °C is assigned to the asymmetric stretching vibration of S=O bonds having a high double bond nature.[25] However, the drastic shift of the IR band from 1376 cm^{-1} to lower wavenumber (not shown due to the overlaps of skeletal vibration bands of ZrO_2) after ammonia adsorption [Figure 7(b)] indicates a strong interaction between an adsorbed ammonia molecule and the surface complex. Namely, the surface sulfur compound in the highly acidic catalysts has a strong tendency to reduce the bond order of SO from a highly covalent double-bond character to a lesser double-bond character when a basic ammonia molecule is adsorbed on the catalysts.[25] Acid

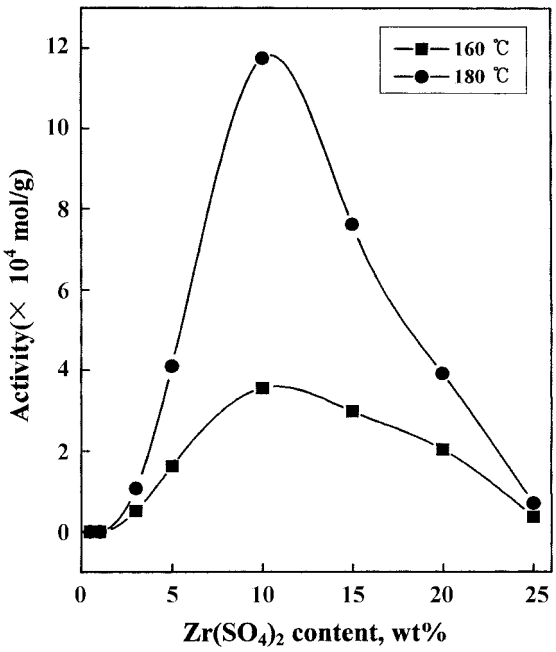

Figure 8. Catalytic activities of $Zr(SO_4)_2/ZrO_2$ for 2-propanol dehydration as a function of $Zr(SO_4)_2$ content.

stronger than $H_o \leq -11.93$, which corresponds to the acid strength of 100% H_2SO_4, are superacids.[1-5,31] The strong ability of the sulfur complex to accommodate electrons from a basic molecule such as ammonia is a driving force to generate superacidic properties.[19,25] Consequently, $Zr(SO_4)_2/ZrO_2$ catalysts would be solid superacids, in analogy with the case of ZrO_2 modified with sulfate group.[18,21,22]

Catalytic activities for acid catalysis. It is interesting to examine how the catalytic activity of acid catalyst depends

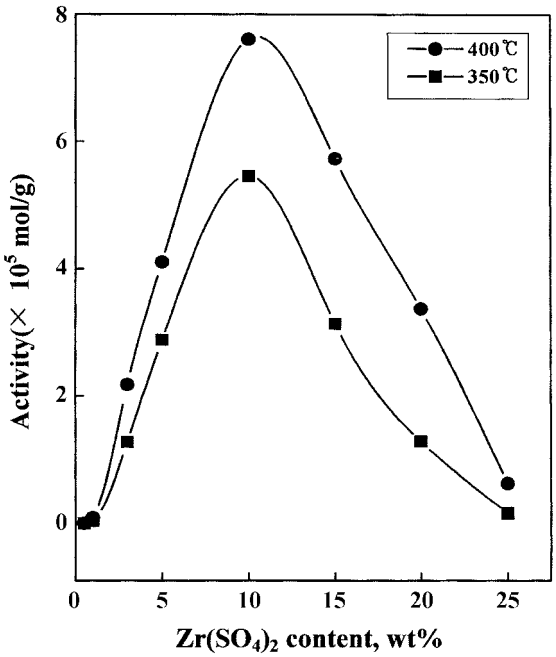

Figure 9. Catalytic activities of $Zr(SO_4)_2/ZrO_2$ for cumene dealkylation as a function of $Zr(SO_4)_2$ content.

on the acid property. The catalytic activities for the 2-propanol dehydration are measured and the results are illustrated as a function of $Zr(SO_4)_2$ content in Figure 8, where reaction temperatures are 160-180 °C. In view of Table 1 and Figure 8, the variations in catalytic activity for 2-propanol dehydration are well correlated with the changes of their acidity, showing the highest activity and acidity for 10-$Zr(SO_4)_2/ZrO_2$. It has been known that 2-propanol dehydration takes place very readily on weak acid sites.[32,33] Good correlations have been found in many cases between the acidity and the catalytic activities of solid acids. For example the rates of both the catalytic decomposition of cumene and the polymerization of propylene over SiO_2-Al_2O_3 catalysts were found to increase with increasing acid amounts at strength $H_o \leq +3.3$.[34] It was also reported that the catalytic activity of nickel silicates in the ethylene dimerization as well as in the butene isomerization was closely correlated with the acidity of the catalyst.[35]

Cumene dealkylation takes place on relatively strong acid sites of the catalysts.[32,33] Catalytic activities for cumene dealkylation against $Zr(SO_4)_2$ content are presented in Figure 9, where reaction temperature is 350-400 °C. Comparing Table 1 and Figure 9, the catalytic activities are also correlated with the acidity. The correlation between catalytic activity and acidity holds for both reactions, 2-propanol dehydration and cumene dealkylation, although the acid strength required to catalyze acid reaction is different depending on the type of reactions. As seen in Figures 8 and 9, the catalytic activity for cumene dealkylation, in spite of higher reaction temperature, is lower than that for 2-propanol dehydration.

Catalytic activities of 10-$Zr(SO_4)_2/ZrO_2$ are plotted as a function of calcination temperature for 2-propanol dehydration in Figure 10. The activities increased with the calcination temperature, giving a maximum at 600 °C and then the activities decreased. Catalytic activities of 10-$Zr(SO_4)_2/ZrO_2$ for cumene dealkylation are also plotted as a function of calcination temperature in Figure 11. The activities also exhibited a maximum at 600 °C. The decrease of activity for both reactions above 600 °C can be probably attributed to the fact that the surface area and acidity above 600 °C decrease with the calcination temperature.

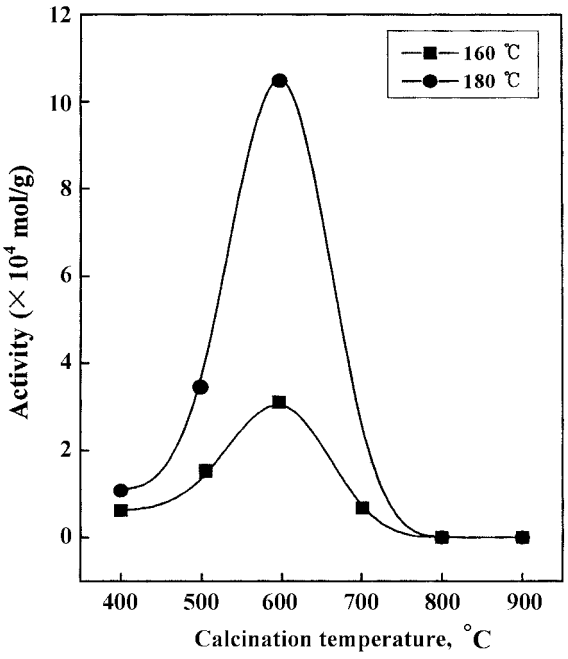

Figure 10. Catalytic activities of 10-$Zr(SO_4)_2/ZrO_2$ for 2-propanol dehydration as a function of calcination temperature.

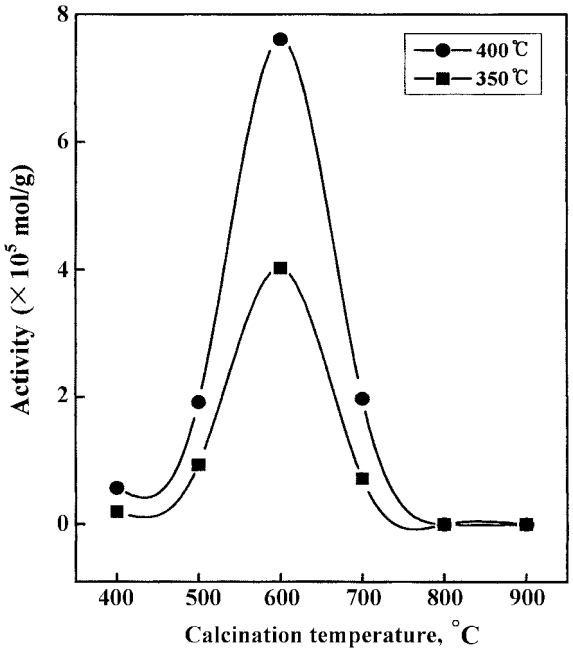

Figure 11. Catalytic activities of 10-$Zr(SO_4)_2/ZrO_2$ for cumene dealkylation as a function of calcination temperature.

Conclusions

This paper has shown that a combination of FTIR, DSC, and XRD can be used to characterize $Zr(SO_4)_2/ZrO_2$ prepared by impregnation of powdered $Zr(OH)_4$ with zirconium sulfate aqueous solution followed by calcining in air. The interaction between zirconium sulfate and zirconia influenced the physicochemical properties of prepared catalysts with calcination temperature. The presence of zirconium sulfate delays the phase transitions of ZrO_2 from amorphous to tetragonal and from tetragonal to monoclinic. The specific surface area and acidity of catalysts increase proportionally with the zirconium sulfate content up to 10 wt % of $Zr(SO_4)_2$ in catalysts. The proportional increment between catalytic acidity and acidity holds for both reactions, 2-propanol dehydration and cumene dealkylation, although the acid strength required to catalyze acid reaction is different depending on the type of reactions.

Acknowledgment. This work was supported by grant NO. (2001-1-30700-006-2) from the Basic Research Program of the Korea Science and Engineering Foundation. We wish to thank Korea Basic Science Institute (Taegu Branch) for the use of X-ray diffractometer.

References

1. Sohn, J. R.; Pae, Y. I.; Jang, H. J.; Park, M. Y. *J. Catal.* **1995**, *127*, 449.
2. Sohn, J. R.; Ryu, S. G. *Langmuir* **1993**, *9*, 126.
3. Kayo, A.; Yamaguchi, T.; Tanabe, K. *J. Catal.* **1983**, *83*, 99.
4. Tanabe, K.; Misono, M.; Ono, Y.; Hattori, H. *New Solid Acids and Base*; Elsevier Science: Amsterdam, 1989; p 27.
5. Arata, K. *Adv. Catal*. **1990**, *37*, 165.
6. Ward, D. A.; Ko, E. I. *J. Catal*. **1994**, *150*, 18.
7. Vaudagna, S. R.; Comelli, R. A.; Canavese, S. A.; Figoli, N. S. *J. Catal*. **1997**, *169*, 389.
8. Kustov, L. M.; Kazansky, V. B.; Figueras, F.; Tichit, D. *J. Catal*. **1994**, *150*, 143.
9. Sayari, A.; Yang, Y.; Song, X. *J. Catal*. **1997**, *167*, 346.
10. Hsu, C. Y.; Heimbuch, C. R.; Armes, C. T.; Gates, B. C. *J. Chem. Soc., Chem. Commun.* **1992**, 1645.
11. Cheung, T. K.; Gates, B. C. *J. Catal*. **1997**, *168*, 522.
12. Hosoi, T.; Shimadzu, T.; Ito, S.; Baba, S.; Takaoka, H.; Imai, T.; Yokoyama, N. *Prepr. Symp. Div. Petr. Chem*. American Chemical Society: Los Angeles, 1988; p 562.
13. Ebitani, K.; Konishi, J.; Hattori, H. *J. Catal*. **1991**, *130*, 257.
14. Signoretto, M.; Pinna, F.; Strukul, G.; Chies, P.; Cerrato, G.; Ciero, S. D.; Morterra, C. *J. Catal*. **1997**, *167*, 522.
15. Hino, M.; Arata, K. *J. Chem. Soc., Chem. Commun*. **1987**, 1259.
16. Larsen, G.; Lotero, E.; Parra, R. D. In *Proc. 11th Int. Congr. Catal*.; Elsevier Science: Amsterdam, 1996; p 543.
17. Arata, K.; Hino, M.; Yamagata, N. *Bull. Chem. Soc. Jpn.* **1990**, *63*, 244.
18. Sohn, J. R.; Park, W. C. *Bull. Korean Chem. Soc.* **2000**, *21*, 1063.
19. Sohn, J. R.; Park, W. C. *Bull. Korean Chem. Soc*. **1999**, *20*, 1261.
20. Sohn, J. R.; Cho, S. G.; Pae, Y. I.; Hayashi, S. *J. Catal*. **1996**, *159*, 170.
21. Sohn, J. R.; Park, M. Y. *J. Ind. Eng. Chem*. **1998**, *4*, 84.
22. Sohn, J. R.; Kim, H. W.; Park, M. Y.; Park, E. H.; Kim, J. T.; Park, S. E. *Appl. Catal. A: General* **1995**, *128*, 127.
23. Saur, O.; Bensitel, M.; Saad, A. B. H.; Lavalley, J. C.; Tripp, C. P.; Morrow, B. A. *J. Catal*. **1986**, *9*, 104.
24. Morrow, B. A.; McFarlane, R. A.; Lion, M.; Lavalley, J. C. *J. Catal*. **1987**, *107*, 232.
25. Yamaguchi, T. *Appl. Catal*. **1990**, *61*, 1.
26. Larsen, G.; Lotero, E.; Petkovic, L. M.; Shobe, D. S. *J. Catal*. **1997**, *169*, 67.
27. Afanasiev, P.; Geantet, C.; Breysse, M.; Coudurier, G.; Vedrine, J. C. *J. Chem. Soc. Faraday Trans*. **1994**, *90*, 193.
28. Sohn, J. R.; Lee, S. Y. *Appl. Catal. A: General* **1997**, *164*, 127.
29. Basila, M. R.; Kantner, T. R. *J. Phys. Chem*. **1967**, *71*, 467.
30. Satsuma, A.; Hattori, A.; Mizutani, K.; Furuta, A.; Miyamoto, A.; Hattori, T.; Murakami, Y. *J. Phys. Chem*. **1988**, *92*, 6052.
31. Olah, F. G. A.; Prakash, G. K. S.; Sommer, J. *Science* **1979**, *206*, 13.
32. Sohn, J. R.; Jang, H. J. *J. Mol. Catal*. **1991**, *64*, 349.
33. Decanio, S. J.; Sohn, J. R.; Paul, P. O.; Lunsford, J. H. *J. Catal*. **1986**, *101*, 132.
34. Tanabe, K. *Solid Acids and Bases*; Kodansha: Tokyo, 1970; p 103.
35. Sohn, J. R.; Ozaki, A. *J. Catal*. **1980**, *61*, 29.